Int. J. Multiphase Flow Vol. 19, No. 6, pp. 1045–1060, 1993
Printed in Great Britain.

0301-9322/93 $6.00 + 0.00

FORCED CONVECTIVE FILM CONDENSATION INSIDE VERTICAL TUBES

S. L. CHEN and M. T. KE
Department of Mechanical Engineering, National Taiwan University, Taipei, Taiwan, R.O.C.

(Received 13 February 1991; in revised form 11 August 1993)

Abstract—A theoretical study of forced convective film condensation inside vertical tubes is presented. We propose a unified procedure for predicting the pressure gradient and condensation heat transfer coefficient of a vapor flowing turbulently in the core and associated with laminar or turbulent film on the tube wall. The analysis for the vapor flows is performed under the condition that the velocity profiles are locally self-similar. The laminar and turbulent film models equate the gravity, pressure and viscous forces, and consider the effect of interfacial shear. The transition from laminar to turbulent film depends not only on the liquid Reynolds number but also on the interfacial shear stress. In this work we also proposed a new eddy viscosity model which is divided into three regions: the inner region in liquid condensate near the wall; the interface region including both liquid and vapor; and the outer region for the vapor core. Comparisons of the theory with some published experimental data showed good agreement.

Key Words: annular film, interfacial shear stress, condensation heat transfer, pressure gradient

1. INTRODUCTION

The phenomenon of film condensation occurs in many practical situations and is of great interest in several technical areas. Many methods have been proposed for predicting the film-condensation heat transfer. The classical Nusselt model (Collier 1972) for film condensation of a quiescent vapor along an isothermal vertical plate equates gravity and viscous forces and assumes a linear temperature profile across the condensate layer and no interfacial shear exerting on the condensate film. However, measured heat transfer coefficients are found to be somewhat larger than those predicted by Nusselt theory. At low film Reynolds numbers, the discrepancy has been attributed to the presence of waves on the film surface (Kutateladze 1982). As forced convective film condensation occurs inside vertical tubes, such a difference is due to the vapor shear stress acting on the vapor–liquid interface.

When saturated vapor flows through a vertical tube, a laminar annular film occurs on the wall. The interfacial shear due to vapor flow tends to accelerate the liquid flow and makes the film thinner. Consequently, the condensation heat transfer is increased. Since the condensate film is thin (curvature effects are negligible), the modified Nusselt analysis (Collier 1972) offers a valid first approximation. Lucas & Moser (1979) used an approximate method to investigate laminar film condensation in tubes. Their results demonstrated that the liquid film thickness is always much smaller than the tube radius for downward vapor flows. Dobran & Thorsen (1979) critically examined both hydrodynamics and heat transfer in a vertical tube under laminar liquid-vapor flow. This analytical approach is helpful for understanding the mechanisms of condensate flow and heat transfer.

Due to the condensation inside a tube, the flowrates of the liquid and vapor change along the tube, altering the pressure gradient and the interfacial shear stress. Even an initially laminar film flow eventually becomes turbulent. Rohsenow *et al.* (1956) showed that the transition from laminar to turbulent flow does not occur at a particular liquid Reynolds number, as in the case for a single-phase flow. The transition depends not only on the liquid velocity and viscosity but also on local flow conditions such as the shear stress distribution in the liquid film.

Numerous experimental data and correlations are available for annular turbulent condensing flows inside vertical tubes. Empirical correlations can be used for practical design without performing complicated calculations. However, most of these correlations do not include sufficient parameters to fully describe the condensate flow, which will limit their applicability. Carpenter &

Colburn's (1951) semi-empirical correlation works well for some fluids. The coefficient and the exponent of the Prandtl number, and the procedure for calculating wall shear stress were modified by Soliman *et al.* (1968) and Altman *et al.* (1960) to generalize their correlations for all fluids. Shah (1979) also gave a refined correlation. Another approach used the momentum and heat transfer analogy. With the correlation of interfacial shear stress determined from the adiabatic cocurrent liquid–vapor flow, Dukler (1960) developed an analysis assuming the existence of the universal velocity distribution.

It is evident that no analytic treatment exists which is free from a semi-empirical approach and which is consistent with the whole process of condensation (including laminar and turbulent film flows) inside a vertical tube. This paper deals with convective filmwise condensation of pure saturated vapor flowing downward inside a vertical tube. A unified procedure is proposed to predict the pressure drop and condensation heat transfer coefficient of turbulent vapor flows associated with laminar or turbulent liquid condensate. This theory compares well with the experimental data in the literature.

2. PHYSICAL MODEL AND FORMULATION

Figure 1 schematically illustrates the condensation process and defines the coordinate system for the problem. A vapor enters the vertical tube turbulently and its velocity profiles are fully developed. The tube surface temperature is cooled to below the saturated temperature. Filmwise condensation occurs along the vertical tube. Laminar film flows on the upper portion of a vertical tube and turbulent film flows on the lower portion.

2.1. Turbulent vapor

The analysis begins with the conservation equations for mass and momentum for turbulent vapor flowing in a circular tube. These may be written as

$$\frac{\partial}{\partial r}(rv_G) + \frac{\partial}{\partial x}(ru_G) = 0 \qquad [1]$$

and

$$\rho_G\left[r\frac{\partial u_G^2}{\partial x} + \frac{\partial}{\partial r}(ru_G v_G)\right] = -r\frac{\partial p}{\partial x} - \frac{\partial}{\partial r}(r\tau_G), \qquad [2]$$

where u_G is the axial velocity, v_G is the transverse velocity, p is the pressure, τ_G is the shear stress, ρ_G is the vapor density, r is the radial coordinate and x is the axial coordinate of the vapor phase. For turbulent flows, it is customary to write the relationship between the shear stress and the velocity gradient in a form equivalent to the following:

$$\tau_G = -\rho_G(\nu_G + \epsilon_M)\frac{du_G}{dr}, \qquad [3]$$

where ϵ_M is the eddy diffusivity for momentum. The associated boundary conditions for the vapor flow are

$$\left.\begin{aligned} &v_G = v_i \text{ and } \tau_G = \tau_i \quad \text{at} \quad r = R - \delta \ (\text{or } y = \delta) \\ &\frac{\partial u_G}{\partial r} = 0 \qquad\qquad\quad \text{at} \quad r = 0 \ (\text{or } y = R), \end{aligned}\right\} \qquad [4]$$

where v_i is the vapor condensation velocity at the interface, τ_i is the interfacial shear stress, R is the tube radius and δ is the film thickness. All these quantities can be determined from the solutions of condensate film. We assume that the film thickness is small compared to the tube radius ($\delta \ll R$) and the mean vapor velocity $\bar{u}_G$ is larger than the interface velocity u_i($\bar{u}_G \gg u_i$). These assumptions are true since the liquid density is much larger than the vapor density. The boundary conditions on the vapor–liquid interface can then be rewritten as

$$\left.\begin{aligned} u_G &\approx 0 \\ v_G &= v_i \end{aligned}\right\} \quad \text{and } \tau_G = \tau_i \quad \text{at } r \approx R. \qquad [5]$$

For a very small condensation velocity, v_i, it can be further assumed that velocity profiles are locally self-similar; i.e.

$$\frac{u_G}{\bar{u}_G} = f\left(\frac{r}{R}\right). \tag{6}$$

As can be seen that, the turbulence model of vapor flows used in the present work incorporates the main features of Kinney & Sparrow's (1970) work but with two important differences. The first difference is that the suction velocity is a result of condensation on the liquid–vapor interface. This velocity depends upon the intensity of heat transfer in the condensate film. The second difference is the inclusion of the effect of interface damping on eddy transport as deduced from gas absorption data, which will be discussed later. A similar approach proposed by Kinney & Sparrow is used to eliminate the pressure gradient in the momentum equation. Following their steps, the integro-differential equation for the turbulent vapor flows can be obtained as

$$\left(1+\frac{\epsilon_M}{\nu_G}\right)\frac{du_G^+}{dy^+} = \frac{r^+}{R^+}\left(\frac{\tau_i}{\tau_w}\right)DN - N\left(\frac{v_i}{\bar{u}_G}\right)\left(\frac{2}{R^+}\right)\left[\int_0^{R^+} u_G^+(R^+ - y^+)\,dy^+ - \int_0^{y^+} u_G^+(R^+ - y^+)\,dy^+\right] \times \frac{u_G^+}{r^+} + 4N\left(\frac{v_i}{\bar{u}_G}\right)\left(\frac{1}{R^+}\right)\left\{\left[1-\left(\frac{r^+}{R^+}\right)^2\right]\int_0^{R^+} u_G^{+2}(R^+ - y^+)\,dy^+ - \int_0^{y^+} u_G^{+2}(R^+ - y^+)\,dy^+\right\}\frac{1}{r^+}, \tag{7}$$

where $u_G^+ = u_G/u^*$, $y^+ = yu^*/\nu_L$, $R^+ = Ru^*/\nu_L$, $y^+ = yu^*/\nu_L$, $u^* = (\tau_w/\rho_L)^{1/2}$, $D = \rho_L/\rho_G$ and $N = \nu_L/\nu_G$; ν_L and ν_G are the kinematic viscosity of liquid and vapor, respectively. Because the vapor condensation process is associated with the surface mass transfer, the vapor pressure gradient, dp/dx, containing both the interfacial shear and momentum flux contributions can be derived as

$$-\frac{\dfrac{dp}{d\left(\dfrac{x}{2R}\right)}}{\dfrac{1}{2}\rho\bar{u}_G^2} = \left[4c_f - 16N^2\left(\frac{v_i}{\bar{u}_G}\right)\frac{8}{Re_G^2}\int_0^{R+} u_G^{+2}(R^+ - y^+)\,dy^+\right], \tag{8}$$

where the vapor Reynolds number Re_G and the friction factor c_f are defined as

$$Re_G = \frac{4N}{R^+}\int_0^{R^+} u_G^+(R^+ - y^+)\,dy^+ \quad \text{and} \quad c_f = 2DN^2\left(\frac{\tau_i}{\tau_w}\right)\left(\frac{2R^+}{Re_G}\right)^2. \tag{9}$$

Where τ_w is the wall shear stress. Equation [7] is a nonlinear integro-differential equation for the axial velocity distributions. The equation will incorporate the film models and turbulent transport model to determine the effect of interfacial shear on film condensation.

2.2. *Laminar film*

Consider the control volume defined in the condensate film in figure 1. For the laminar flow case, neglecting inertia effects, a balance of the shear, gravity and pressure forces on the control volume yields the expression for the condensate velocity along the tube wall as

$$u_L = \frac{(\rho_L - \rho_G)g}{\mu_L}G\left(\delta y - \frac{1}{2}y^2\right) + \frac{\tau_i}{\mu_L}y, \tag{10}$$

where g is the gravity acceleration, μ_L is the dynamic viscosity of the liquid and G is defined as

$$G = 1 - \frac{1}{(\rho_L - \rho_G)g}\frac{dp}{dx}. \tag{11}$$

The continuity requires

$$\frac{(\rho_L-\rho_G)g}{3\nu_L}G\delta^3+\frac{\tau_i}{2\nu_L}\delta^2-\Gamma=0, \tag{12}$$

where Γ is the mass flowrate of liquid per unit periphery ($\Gamma=m_L/2\pi R$). This expression is a modified Nusselt analysis for condensation inside a tube, including the effect of vapor shear stress in the interface. With the help of the definition of film Reynolds number (defined as $Re_L=4\Gamma/\mu_L$) and $\rho_L\gg\rho_G$, [12] yields an implicit equation for δ^* (defined as $\delta^*=\delta/(\nu_L^2/g)^{1/3}$) in terms of dimensionless interfacial shear stress τ_i^* (defined as $\tau_i^*=\tau_i/[(\rho_L-\rho_G)(\nu_L g)^{2/3}]$):

$$Re_L\left(1-\frac{1}{D}\right)^{-1}=\frac{4}{3}G\delta^{*3}+2\tau_i^*\delta^{*2}. \tag{13}$$

The local value of the laminar heat transfer coefficient h_L is determined from the energy balance in the tube wall:

$$-k_L\frac{dT}{dy}\bigg|_w=h_L(T_{sat}-T_w), \tag{14}$$

where k_L is the thermal conductivity, T is the temperature, T_{sat} is the saturation temperature and T_w is the wall temperature of liquid film. Since the temperature profile across the condensate is linear, the local condensation heat transfer coefficient becomes

$$h_L=\frac{k_L}{\delta}. \tag{15}$$

It is convenient to introduce the film Nusselt number as

$$Nu_L=\frac{h_L\left(\frac{\nu_L^2}{g}\right)^{1/3}}{k_L}=\frac{1}{\delta^*}. \tag{16}$$

2.3. Transition from laminar to turbulent film

For long vertical tubes it is possible to obtain an Re_L which exceeds the critical value at which turbulence begins. In the absence of vapor shear stress, McAdams (1954) suggested the transition from laminar to turbulent films occurs when $Re_L=1800$. With a significant vapor shear stress, there are very few good data available to establish the conditions under which transition occurs. For this reason, we use the correlations developed by Rohsenow *et al.* (1956). They found the transition to occur at:

(1) for moderate values of $\tau_i^*\left[\tau_i^*<\dfrac{11.05}{\left(1-\frac{1}{D}\right)^{1/3}}\right]$,

$$(Re_L)_t=1800-246\left(1-\frac{1}{D}\right)^{1/3}\tau_i^*+0.667\left(1-\frac{1}{D}\right)(\tau_i^*)^3; \tag{17}$$

and

(2) for very high values of $\tau_i^*\left[\tau_i^*>\dfrac{11.05}{\left(1-\frac{1}{D}\right)^{1/3}}\right]$,

$$(Re_L)_t\left(1-\frac{1}{D}\right)^{-1}=\frac{4}{3}G(\delta_t^*)^3+2\tau_i^*(\delta_t^*)^2 \tag{18}$$

where δ_t^* satisfies

$$G(\delta_t^*)^3+(\tau_i^*)(\delta_t^*)^2=\frac{36}{1-\frac{1}{D}}. \tag{19}$$

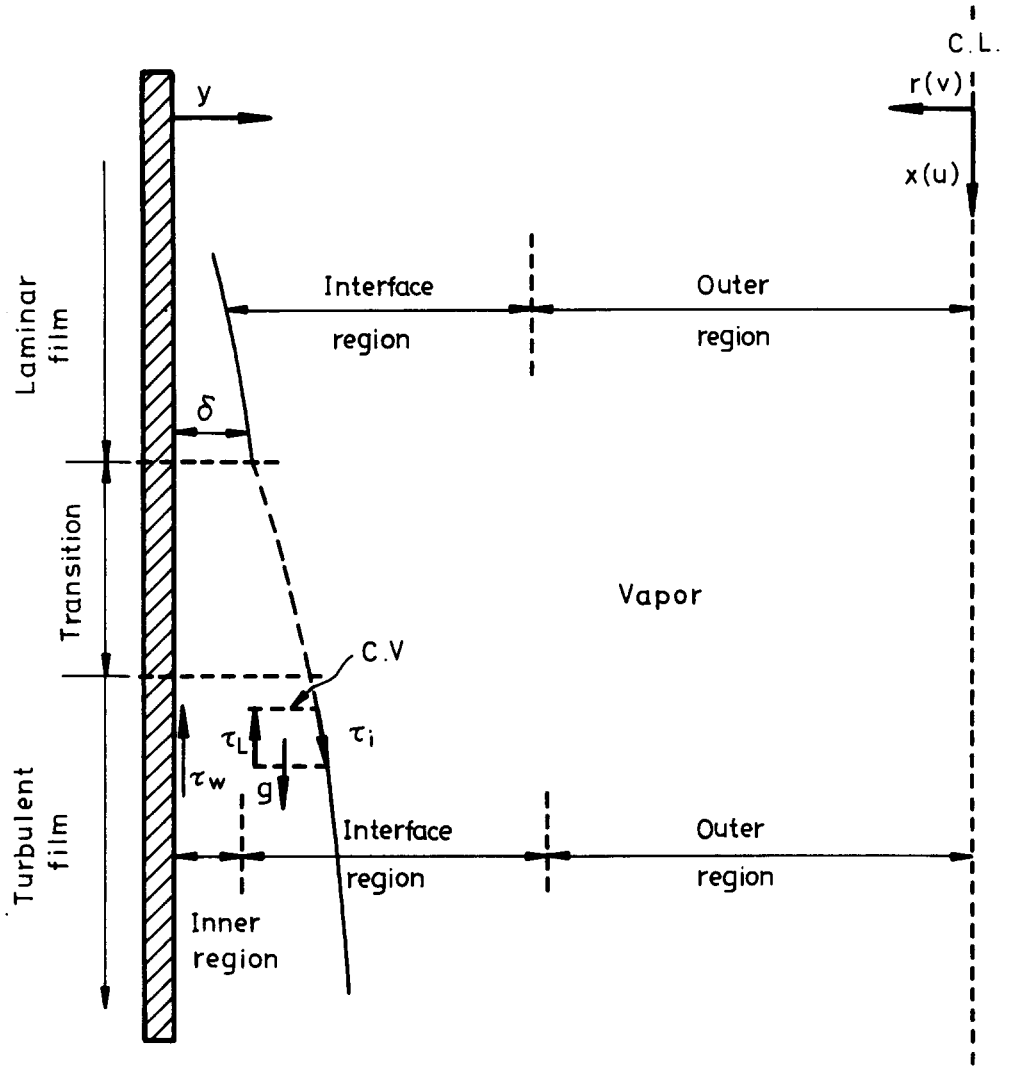

Figure 1. Filmwise condensation in a vertical tube.

2.4. *Turbulent film*

For turbulent flow of the condensate layer, a force balance on the control volume defined in figure 1 gives the total shear distribution:

$$\tau_L = \left[(\rho_L - \rho_G)g - \frac{dp}{dx}\right](\delta - y) + \tau_i. \qquad [20]$$

The wall shear stress is $\tau_w = [(\rho_L - \rho_G)g - (dp/dx)]\ \delta + \tau_i$. If we define

$$s^3 = \frac{(\rho_L - \rho_G)Gg\delta}{\tau_w} = \frac{\delta^{*3}}{\delta^{+2}}, \qquad [21]$$

where δ^+ is defined as $y^+ = yu^*/\nu_L$. Substitute the relationship between the shear stress and the velocity gradient into [20]. The universal velocity distribution can be obtained as

$$\frac{du_L^+}{dy^+} = \frac{1 - \dfrac{s^3 y^+}{\delta^+}}{1 + \dfrac{\epsilon_M}{\nu_L}}, \qquad [22]$$

where $\tau_L/\tau_w = 1 - s^3 y^+/\delta^+$ and $u_L^+ = u_L/u^*$.

The energy equation for the turbulent film is represented in dimensionless form as

$$\frac{\partial}{\partial\eta}\left[\left(1+\frac{\epsilon_H}{\nu_L}\mathrm{Pr}_L\right)\frac{\partial\theta}{\partial\eta}\right]=0, \qquad [23]$$

where ϵ_H is the thermal eddy diffusivity, Pr_L is the liquid Prandtl number and $\eta = y/\delta$. The nondimensional temperatures, θ, associated with the boundary conditions of constant wall heat flux or constant wall temperature, are defined as

$$\theta=\frac{T-T_{sat}}{\frac{q_w\delta}{k_L}} \quad \begin{cases}\eta=0 & \dfrac{\partial\theta}{\partial\eta}=-1\\ \eta=1 & \theta=0\end{cases} \quad \text{(constant wall heat flux)} \qquad [24]$$

and

$$\theta=\frac{T-T_w}{T_{sat}-T_w} \quad \begin{cases}\eta=0 & \theta=0\\ \eta=1 & \theta=1\end{cases} \quad \text{(constant wall temperature).} \qquad [25]$$

Where q_w is the wall heat flux. Equation [23] can be integrated to give the dimensionless temperature distributions. For the case of film condensation at constant wall heat flux

$$\theta=\int_\eta^1\frac{d\eta}{1+\frac{\epsilon_H\,\mathrm{Pr}_L}{\nu_L}}. \qquad [26]$$

The heat transfer coefficient is defined as $h_L = q_w/(T_w - T_{sat})$. The film Nusselt number can be expressed as

$$\mathrm{Nu}_L=\frac{1}{\delta^*}\int_0^1\frac{d\eta}{1+\frac{\epsilon_H\,\mathrm{Pr}_L}{\nu_L}}. \qquad [27]$$

For the case of constant wall temperature, we can integrate [23] and obtain the temperature distribution as

$$\theta=\int_0^\eta\frac{C}{1+\frac{\epsilon_H\,\mathrm{Pr}_L}{\nu_L}}d\eta, \qquad [28]$$

where

$$C=\left(\int_0^1\frac{d\eta}{1+\frac{\epsilon_H\,\mathrm{Pr}_L}{\nu_L}}\right)^{-1}. \qquad [29]$$

The heat transfer coefficient of condensation is defined as $h_L = (-k\partial T/\partial y)|_w)/(T_w - T_{sat})$. Therefore, the film Nusselt number is

$$\mathrm{Nu}_L=\frac{1}{\delta^*}\frac{1}{\int_0^1\frac{d\eta}{1+\frac{\epsilon_H\,\mathrm{Pr}_L}{\nu_L}}}. \qquad [30]$$

From the energy balance at the vapor–liquid interface, the vapor condensation velocity can be expressed as

$$v_i=\frac{h_L(T_{sat}-T_w)}{\rho_G h_{fg}} \qquad [31]$$

Where h_{fg} is the latent heat of evaporization. Equation [31] can be expressed in dimensionless form as

$$v_i^+ = \frac{\mathrm{Ja}}{\mathrm{Pr}} \frac{D}{(\tau_w^*)^{1/2}} \mathrm{Nu_L}, \qquad [32]$$

where $\mathrm{Ja} = c_{pL}(T_{sat} - T_w)/h_{fg}$ is the Jacob number and c_{pL} is the specific heat of liquid.

2.5. *Turbulent transport model*

To compute the vapor velocity, [7] condensate velocity, [22] and the film Nusselt number, [27] or [30] would require a specification of an appropriate turbulence model for ϵ_M and ϵ_H in the vapor flow and liquid film. However, the phenomena of eddy transport in two-phase flow are not well understood yet; it is difficult to claim which turbulence model is most appropriate. In this work we propose a new eddy distribution for momentum for annular-film flows, as shown in figure 1. For a laminar film with turbulent vapor flow, an interface region and outer region in the vapor are considered. For the case of a turbulent film with turbulent vapor flow, three regions are included: (1) the inner region for the liquid condensate near the wall; (2) the interface region including both condensate and vapor; and (3) the outer region for the vapor core.

(1) The inner region. Near the tube wall the turbulent film exists as a laminar sublayer. We use the modified van Driest model for a turbulent film used by Yih & Liu (1983). They modified the turbulence model proposed by Limberg (1973) and Seban & Faghri (1976) to include the interfacial shear through the variable shear stress and damping terms. The eddy distribution can be written as

$$\frac{\epsilon_M}{\nu_L} = -0.5 + 0.5\left\{1 + 0.64y^{+2}\frac{\tau_L}{\tau_w}\left[1 - \exp\left(\frac{-y^+\left(\frac{\tau_L}{\tau_w}\right)^{1/2}}{25.1}\right)\right]^2 f^2\right\}^{1/2}, \qquad [33]$$

where $\tau_L/\tau_W = 1 - s^3y^+/\delta^+$ and $f = \exp[-1.66(1 - \tau_L/\tau_W)]$ is a damping factor.

(2) The interface region. In this region condensation occurs in the liquid–vapor interface. We use an interface damping eddy diffusivity model as deduced from the gas absorption data of Lamourelle & Sandall (1972). Mills & Chung (1973) further modified their eddy diffusivity model at the liquid–vapor interface region of film evaporation:

$$\frac{\epsilon_M}{\nu} = 6.47 \times 10^{-4}\frac{g\rho}{\sigma}\left(\frac{\nu_L}{u^*}\right)^2(\delta^+ - y^+)^2\,\mathrm{Re}^{1.678}, \qquad [34]$$

where σ is the surface tension. In [34] the physical properties of the working fluid (such as density) and the Reynolds number depend on its state of liquid or vapor.

(3) The outer region. In the region of the vapor turbulence core, we use the familiar Prandtl–Nikuradze model (Seban 1954; Rohsenow *et al.* 1956) for the outer region:

$$\frac{\epsilon_M}{\nu_G} = \frac{y^+}{2.5}. \qquad [35]$$

The complete ϵ_M profile can be obtained easily by combining [33]–[35] and their intersections are regarded as the separation of each zone, as shown in figure 2. It is noted that there is a discontinuity at the liquid–vapor interface.

The turbulent Prandtl number $\mathrm{Pr_t}$ for the turbulent film is evaluated from Cebeci's modification of the van Driest model and is further modified by Yih & Liu (1983) to include the effect of variable shear:

$$\mathrm{Pr_t} = \frac{\epsilon_M}{\epsilon_H} = \frac{1 - \exp\left[-y^+\left(\frac{\tau_L}{\tau_w}\right)^{1/2}\Big/\mathrm{A}^+\right]}{1 - \exp\left[-y^+\left(\frac{\tau_L}{\tau_w}\right)^{1/2}\Big/\mathrm{B}^+\right]}, \qquad [36]$$

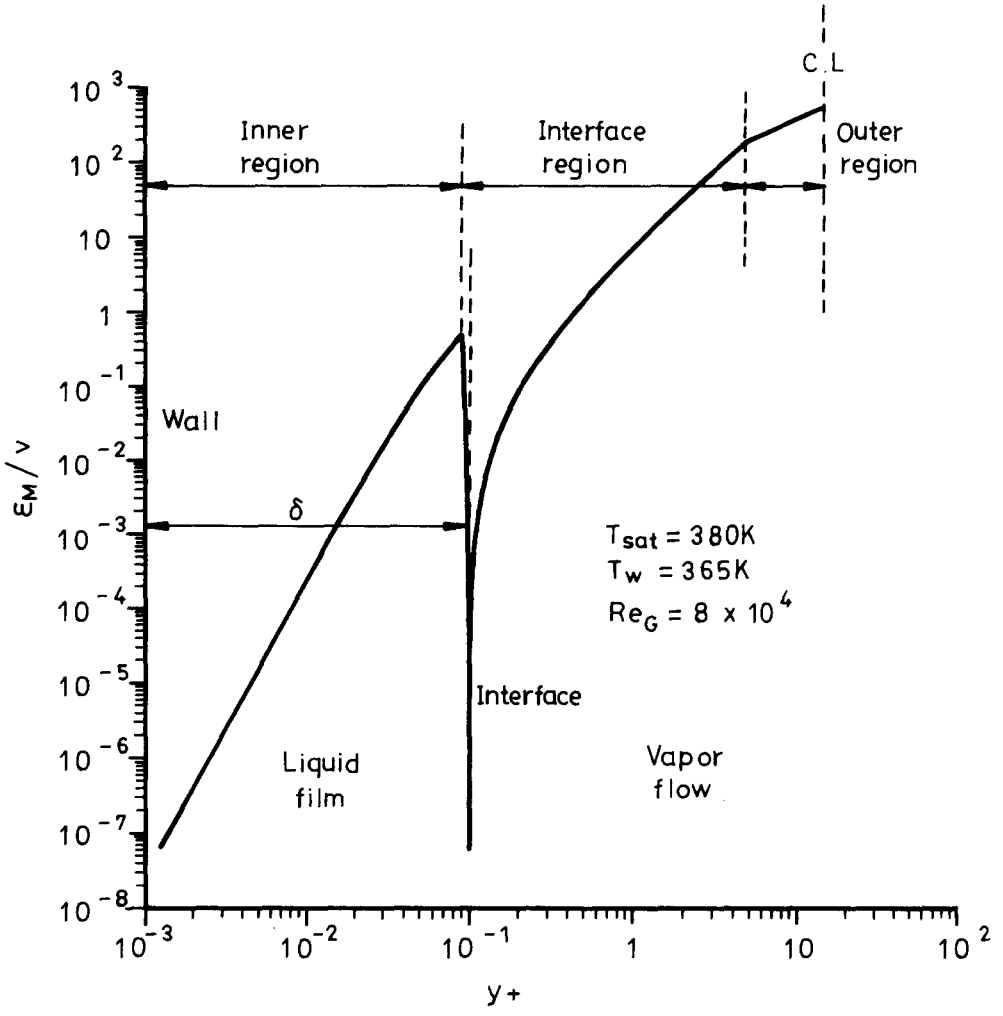

Figure 2. The complete ϵ_M profile inside the liquid film and vapor flow.

where B^+ is given by Habib & Na (1974) as

$$B^+ = Pr^{-1/2} \sum_{i=1}^{5} C_i (\log_{10} Pr)^{i-1}, \qquad [37]$$

and where $C_1 = 34.96$, $C_2 = 28.97$, $C_3 = 33.95$, $C_4 = 6.33$ and $C_5 = -1.186$. Equation [37] reveals the $Pr_t > 1$ near the wall, but approaches 1 as $y^+ \to \delta^+$.

2.6. *Calculation procedures*

First select a value of the vapor Reynolds number and assume the appropriate v_i^+, δ^+ and R^+ for the given Re_{Gin}. These values are substituted into [34] and [35] to obtain the vapor eddy diffusivity for momentum, and then solve for the vapor velocity profile, $u_G^+(y^+)$, from [7]. Thus, dp/dx and δ^* can be obtained from [8] and [12]. Then we can calculate the transition film Reynolds numbers which determine the film flow pattern. If the film is laminar, the Nusselt number is the inverse of the dimensionless film thickness and the vapor condensation velocity v_i^+ can be obtained from [32]. For a turbulent film, the liquid eddy diffusivity for momentum (form [33] and [34]) and s (from [21]) can be obtained. Then solve the liquid velocity profile, $u_L^+(y^+)$, from [22]. The Nusselt number is obtained from [27] or [30] depending on the boundary condition, once ϵ_H is evaluated from [36] and [37]. Substitute these results to obtain v_i^+ from [32] and then iterate the above procedure until all the relative errors are within the given tolerance. In the meantime we should check Re_L from [13] and the modified δ^+ to ensure the continuity. After the local heat transfer

results are obtained, we can determine the vapor Reynolds number for the next section from the overall mass balance.

3. RESULTS AND DISCUSSION

Figure 3 shows the distributions of dimensionless velocity, u_G^+ [in figure 3(a)] and v_G^+ [in figure 3(b)], along the condenser for vapor ($Pr_L = 1.34$) at $Re_{Gin} = 3 \times 10^5$. In all calculations the film thickness is always $<1\%$ of the tube radius. The liquid velocity distributions across the condensate are not shown in this figure because of their small scales. Following the assumption of inlet vapor, the velocity profile in the inlet is fully developed. As the vapor condenses, the flowrate of the vapor is reduced and the axial velocity profiles are locally self-similar and flattened along the condenser. The radial velocity distributions v_G^+ shown in figure 3(b) demonstrate the effect of condensation on the vapor phase. The maximum velocity occurs on the interface (near the wall) and this value becomes smaller as the condensation proceeds. It is obvious that the condensation heat transfer coefficients are decreasing along the condenser.

In order to assess the range of validity of the proposed theoretical model, it is necessary to test the model against experimental data. Surprisingly, there are relatively few complete and reliable experimental data on the condensation of pure vapor in vertical tubes. An examination of the available sources from the literature leads to the selection of data taken from work carried out by Goodykoontz & Dorsch (1966, 1967) and Mochizuki *et al.* (1984). Goodykoontz and Dorsch's data are for the condensation of high velocity steam in downflow through 15.88 and 7.44 mm bore copper tubes. Their data set has the advantage of presenting detailed data. The data from Mochizuki *et al.* are for convective filmwise condensation of R11 and R114 flowing downward inside a vertical tube of 13.9 mm dia. Their data give the local derived values of quality and the heat transfer coefficient presented in graphic form.

Figures 4 and 5 present the comparison between the theory and the experimental data obtained by Goodykoontz & Dorsch (1966, 1967) for low and high velocity steam under the conditions of $T_w = 382$ K and $q_w = 5.49 \times 10^5$ W/m^2. Figure 4 shows the results of the local condensation heat transfer coefficients, while the calculated wall heat flux or wall temperature and pressure gradient are illustrated in figures 5(a) and 5(b), respectively. The data shown in figures 4 and 5 are only small samples from the very large data set obtained in the NASA experiments. The data set chosen here demonstrates some of the interesting features. As can be seen from these figures, the general trend of the data compares well with the theory predictions. However, there are significant deviations in the entrance region (where the quality is highest) and the outlet region (where the quality approaches zero). It is believed that in the entrance region high vapor flowrates, and subsequent vapor shear stress, may cause high entrainment of liquid drops or even breakdown of a continuous liquid film. Predictions from the present model can be in substantial error in this mist–annular flow regime. Since the condensing tube is long enough to allow complete condensation to occur, the flow pattern will change from annular-film flow to nonannular flow (i.e. slug flow). In nonannular flow the heat transfer mechanisms are much more complicated. The present model is no longer applied.

In figure 6, experimental data from Mochizuki *et al.* (1984) are used to check the theory. During the process of condensation, the heat flux remains constant along the condenser [$q_w = 2.2 \times 10^4$ W/m^2 for R11 in figure 6(a) and $q_W = 1.5 \times 10^4$ W/m^2 for R114 in figure 6(b)]. These plots represent the local condensation heat transfer coefficients, quality and wall temperature along the condenser for R11 and R114. Predictions from the present model are also shown in this figure. The dotted line in figure 6(b) represents the film transition from laminar to turbulent. For the high-quality region ($x/D < 120$), the present prediction seems to fit reasonably with the data. However, in the region of $x/D > 120$, the present prediction is lower than the data. Therefore, it can be said that the present model for forced convective film condensation inside vertical tubes can predict qualitatively the behavior of a real process and the quantitative agreement is easily seen in the high-quality region.

Figure 7 demonstrates the effect of interfacial shear stress on film condensation heat transfer coefficients along the condenser for the case of constant wall temperature. We chose the

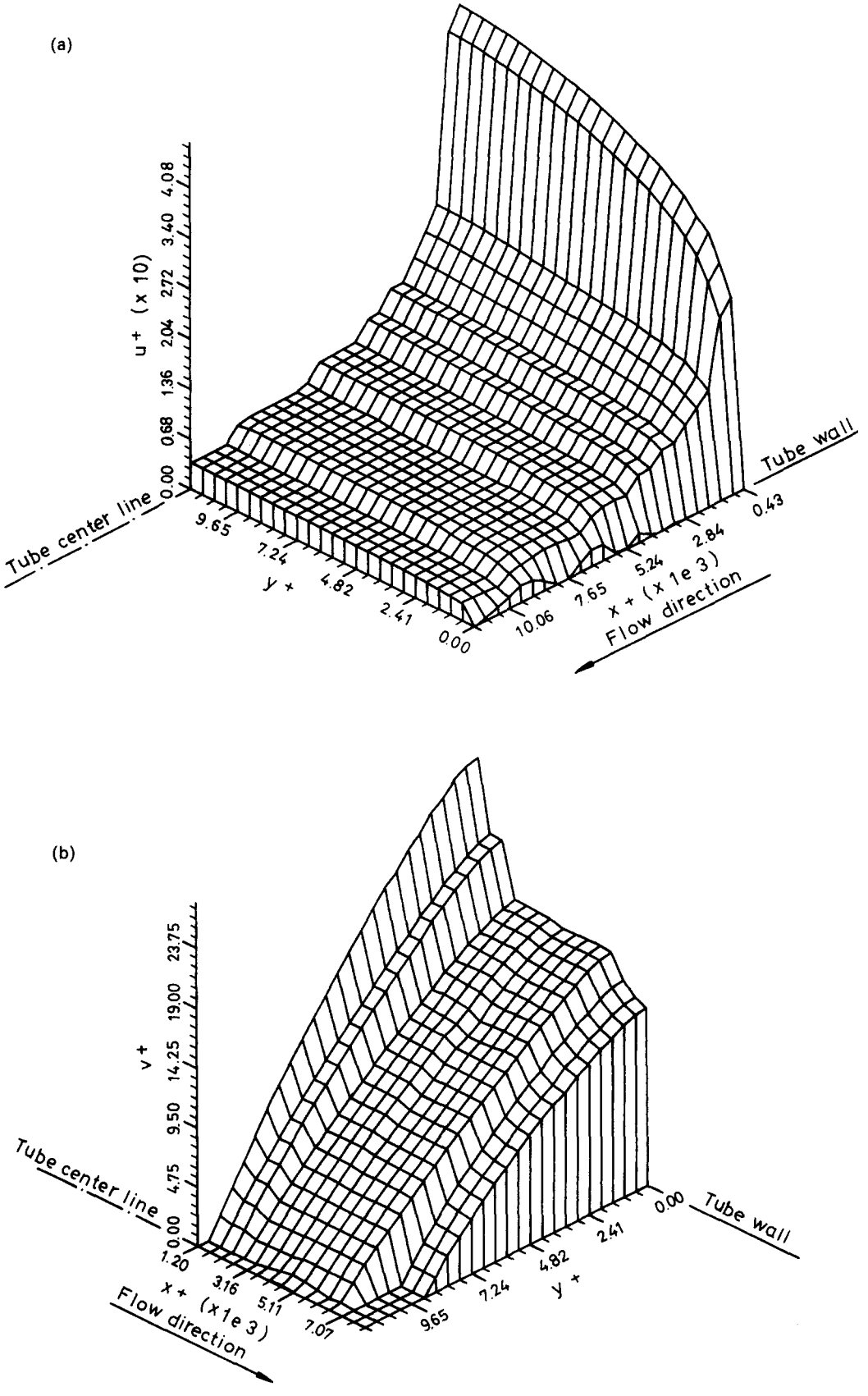

Figure 3. (a) Axial velocity and (b) radial velocity distributions of vapor flow along the condenser.

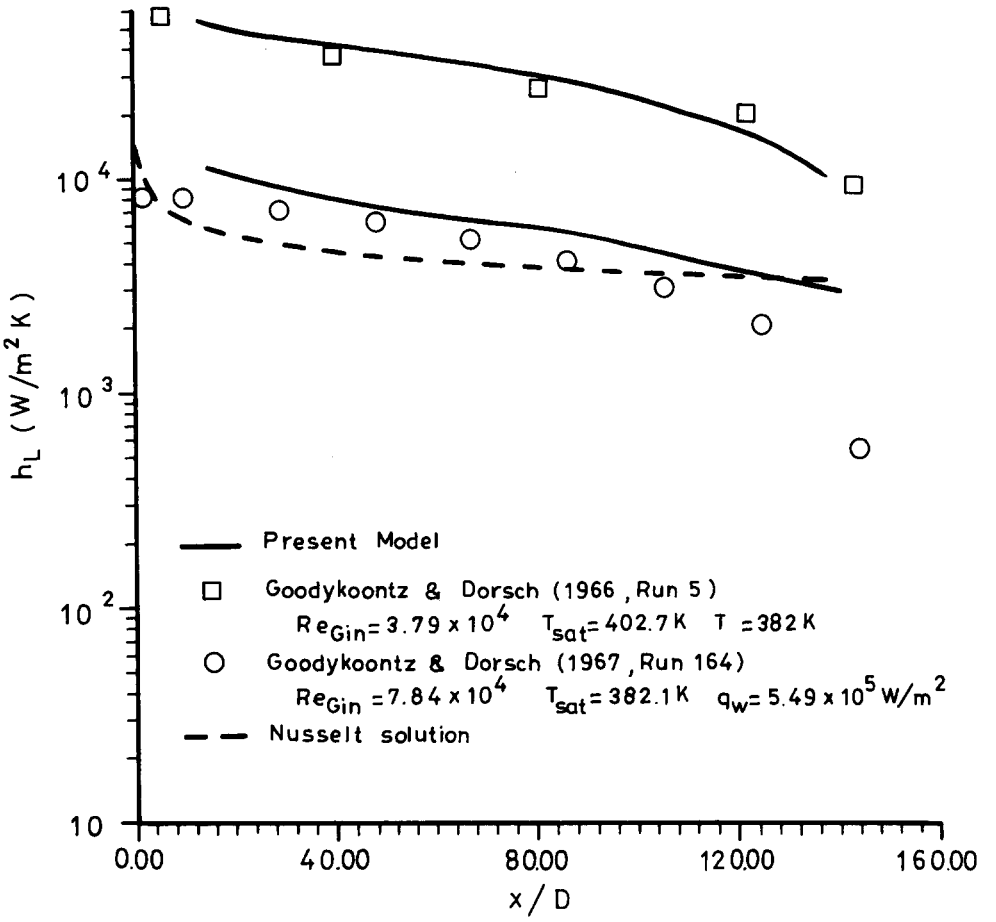

Figure 4. Comparison of the local heat transfer coefficients measured by Goodykoontz & Dorsch (1966, run 5) for low steam velocity and Goodykoontz & Dorsch (1967, run 164) for high velocity steam with the predictions of the present model.

condensation condition encountered practically for condensing steam of $T_{sat} = 100°C$ and $p = 1$ bar with $\rho_L/\rho_G = 1623.8$ and $\nu_L/\nu_G = 27$. The Re_{Gin} ranged from 3×10^4 to 3×10^5. Due to condensation inside the tube, the flowrates of liquid and vapor change along the tube, altering the pressure gradient, the interfacial shear stress and thus the heat transfer coefficients. The results for film flows cover the laminar and turbulent–film regimes. It can be seen that the transition from laminar to turbulent occurs early for higher Re_{Gin}. For the case of lower Re_{Gin} (3×10^4 and 6×10^4 in figure 7), the film flows are laminar. The calculation results also show that the increase in heat transfer by the interfacial shear stress is significant at higher Re_{Gin}. For comparison, Nusselt's theoretical solution is also shown in this figure. It is obvious that Nusselt theory underpredicts the condensation heat transfer coefficients due to the neglect of the interfacial shear.

It is noted that the discontinuities in the figures result from the numerical computations. For a condensation process of pure vapor flowing inside a vertical tube, near the leading edge the liquid film is almost smooth (laminar). Initiated by room distrubances, the liquid film becomes unstable at certain locations and ripples occur at the line of wave inception and periodic waves are then observed. At high Re_L, the dynamical state of this wave flow regime appears to be random and three-dimensional. In between there is the intermediate-wave regime. At much higher Re_L the wavy motion become turbulent. Therefore the transition point where a laminar film turns into a turbulent film can not be exactly computed. The instability of a liquid film is very complicated and is still under study. In the present work, the transition of the liquid film from laminar to turbulent is determined from Re_L and interfacial shear, which cause the discontinuities shown in figures 7 and 8.

In figure 8, we give our results for the dimensionless vapor pressure gradient inside a vertical tube. As can be seen from [8], the vapor pressure gradient is affected by changes in the momentum flux as well as by the interfacial shear (the gravitational pressure gradient is considered to be negligible). As the condensation occurs at the wall, the momentum change of the vapor flow tends to increase the pressure in the flow direction, while the interfacial shear stress tends to cause a

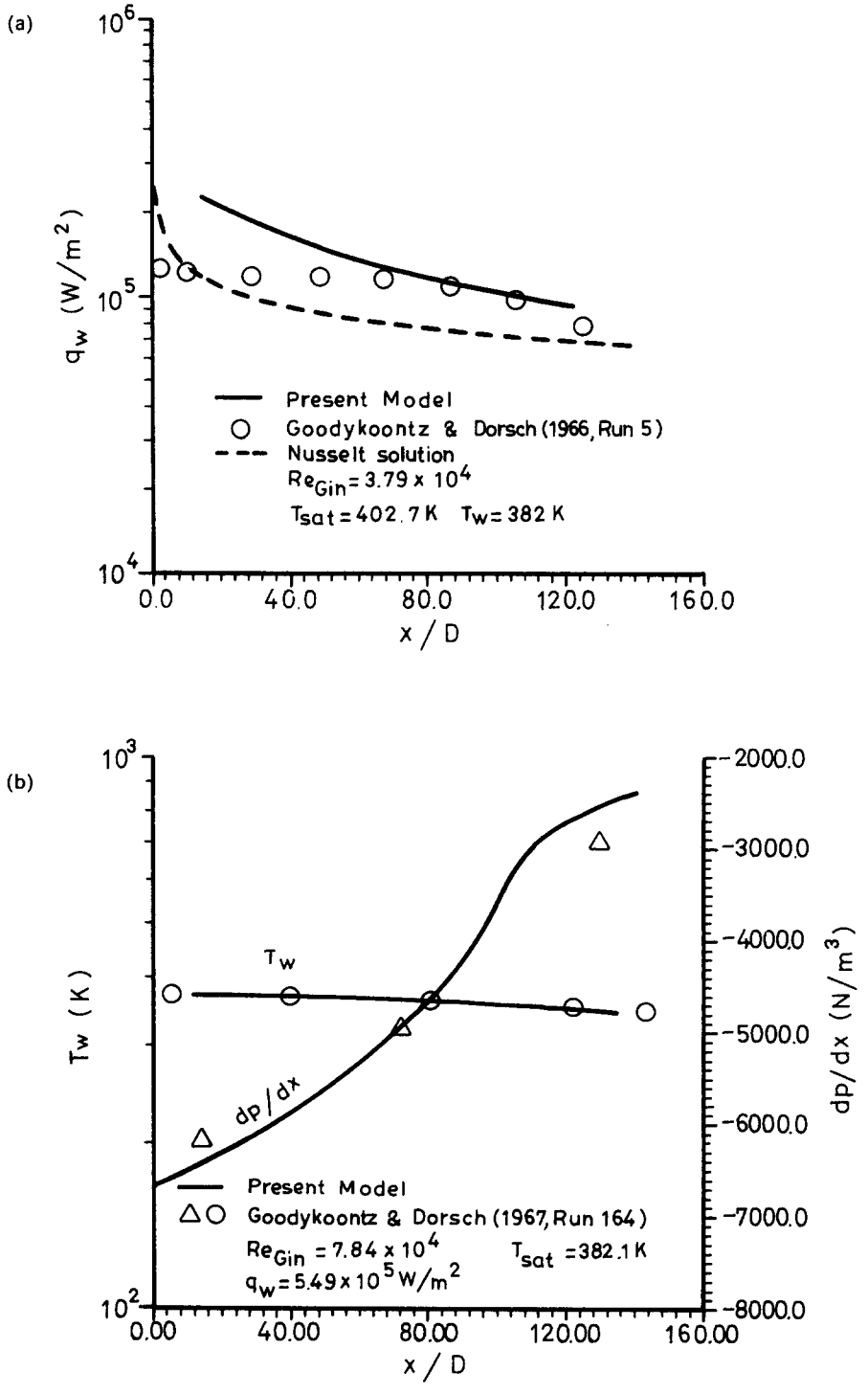

Figure 5. Comparison of (a) the wall heat flux obtained from Goodykoontz & Dorsch (1966, run 5) for low velocity steam and (b) the wall temperature and pressure gradient obtained from Goodykoontz & Dorsch (1967, run 164) for high velocity steam with the predictions of the present model.

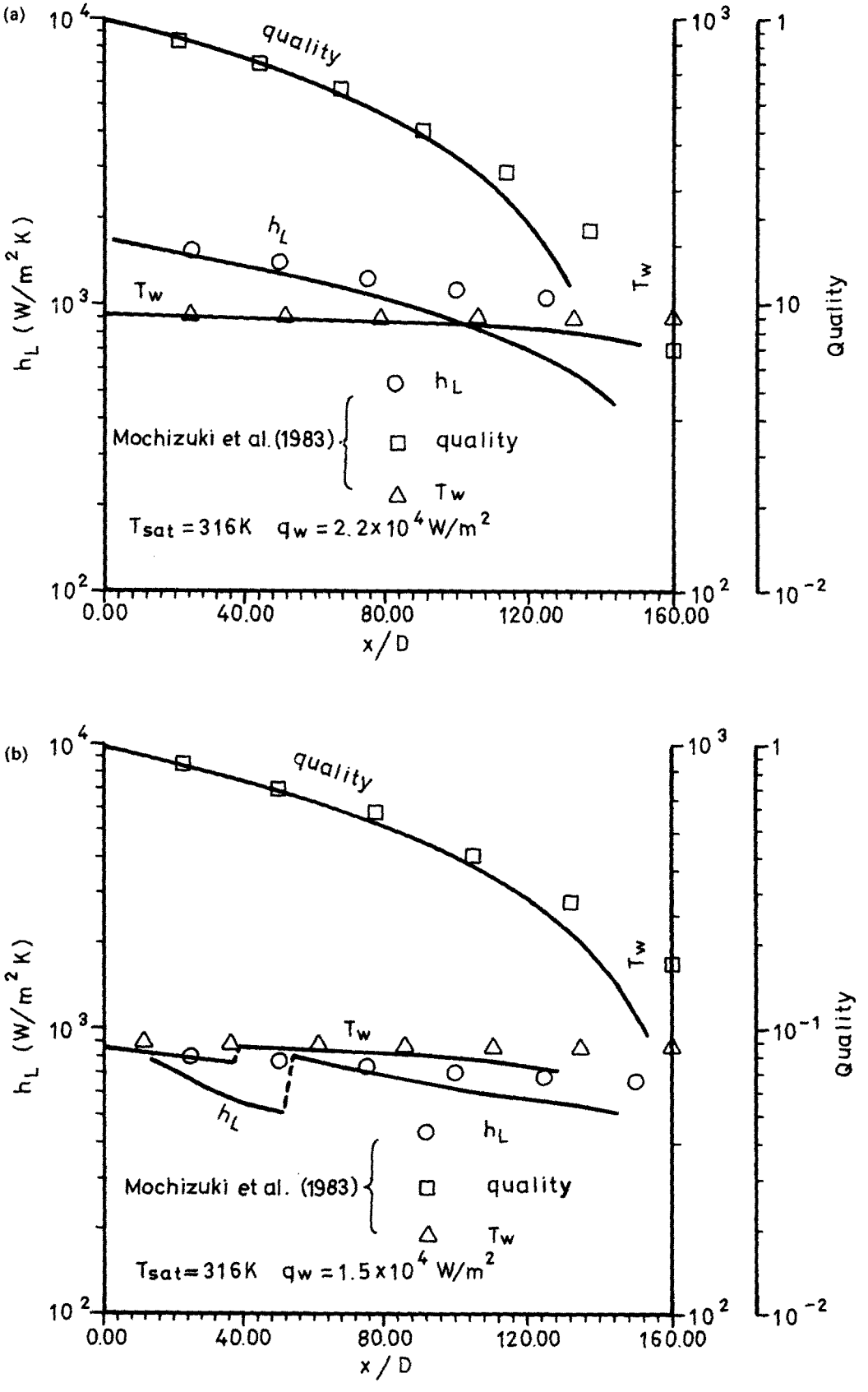

Figure 6. Comparison of the experimental data from Mochizuki *et al.* (1984) with the predictions of the present model: (a) $q_w = 2.2 \times 10^4$ W/m^2 for R11; (b) $q_w = 1.5 \times 10^4$ W/m^2 for R114.

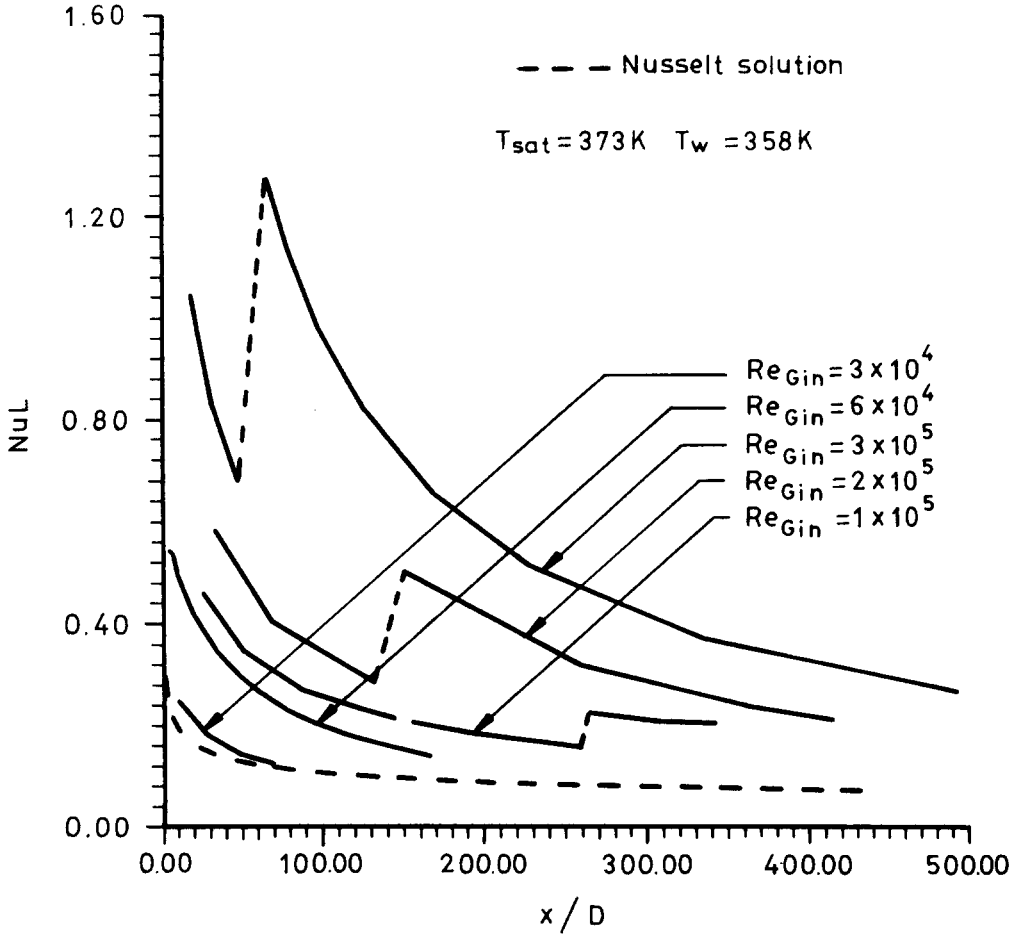

Figure 7. The effect of Re_{Gin} on Nusselt numbers along the condenser.

decrease in pressure. Thus, at any given location, the pressure gradient is affected by the local condensation heat flux. Though figure 8 gives the pressure gradient as a function of Re_{Gin} along the condenser. A sharp change in the pressure gradient deonstes the transition from laminar to turbulent. For the case of $Re_{Gin} = 3 \times 10^5$, dp/dx changes sign and becomes positive when the transition occurs. This behavior indicates that the momentum change due to condensation overcomes the friction caused by the interfacial shear as the flow becomes turbulent.

4. CONCLUSIONS

A theoretical study of filmwise, annular condensation of a saturated vapor in turbulent forced flow through a vertical tube has been conducted in order to reveal the effects of interfacial shear stress on the heat transfer. Comparison with experimental data verify that this theory is capable of predicting the heat transfer coefficient and pressure drop for most liquid–vapor flow regions. It was found that the interfacial shear stress due to the vapor flows has significant effects on the condensation heat transfer and the pressure gradient. Further studies can extend the present model to take into account the effects of superheat vapor or noncondensible gas on forced convective filmwise condensation inside vertical tubes.

Acknowledgements—The authors gratefully acknowledge the support of the National Science Council, R.O.C., for this work through Grant No. NSC-80-0401-E002-11.

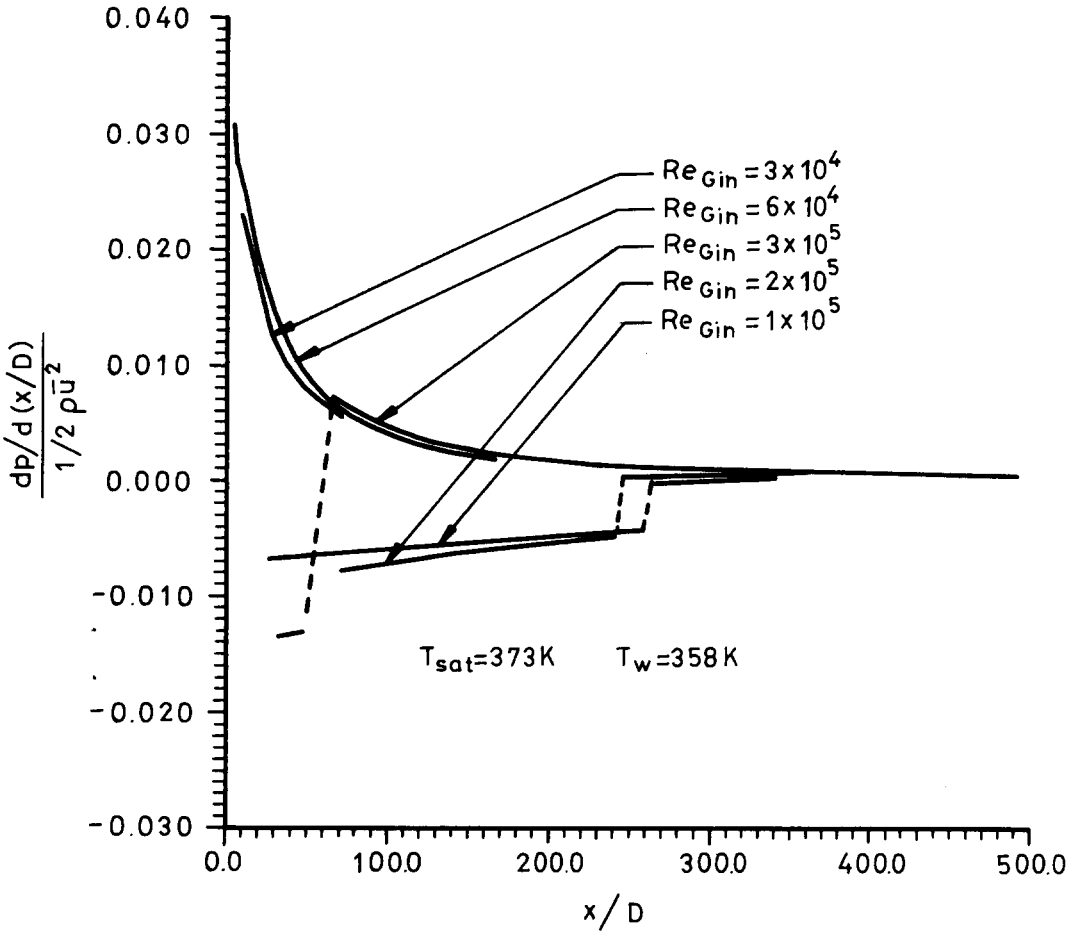

Figure 8. Variation of the local pressure gradient with Re_{Gin} along the condenser.

REFERENCES

ALTMAN, M., STAUB, F. W. & NORRIS, R. H. 1960 Local heat transfer and pressure drop for refrigerant-22 condensing in horizontal tubes. *Chem. Engng Prog. Symp. Ser.* **30,** 151–159.

CARPENTER, E. F. & COLBURN, A. P. 1951 The effect of vapor velocity on condensation inside tubes. In *Proc. General Discussion on Heat Transfer*, pp. 20–26. IMECHE/ASME, New York.

COLLIER, J. G. 1972 *Convective Boiling and Condensation*, Chap. 10. McGraw-Hill, New York.

DOBRAN, F. & THORSEN, R. S. 1979 Forced flow laminar filmwise condensation of a pure vapor in a vertical tube. *Int. J. Heat Mass Transfer* **23,** 161–177.

DUKLER, A. E. 1960 Fluid mechanics and heat transfer in a vertical falling film system. *Chem. Engng Prog. Symp. Ser.* **30,** 1–10.

GOODYKOONTZ, J. H. & DORSCH, R. G. 1966 Local heat-transfer coefficients for condensation of steam in vertical down flow with 5/8 in. diameter tube. Report NASA TN D3326.

GOODYKOONTZ, J. H. & DORSCH, R. G. 1967 Local heat-transfer coefficients and static pressures for condensation of high velocity steam within a tube. Report NASA TN D3953.

HABIB, I. S. & NA, T. Y. 1974 Prediction of heat transfer in turbulent pipe flow with constant wall temperature. *Trans. ASME Jl Heat Transfer* **96C,** 253–254.

KINNEY, R. B. & SPARROW, E. M. 1970 Turbulent flow, heat transfer, and mass transfer in a tube with surface suction. *ASME Jl Heat Transfer* **92,** 117–124.

KUTATELADZE, S. S. 1982 Semi-empirical theory of film condensation of pure vapors. *Int. J. Heat Mass Transfer* **25,** 653–660.

LAMOURELLE, A. P. & SANDALL, O. C. 1972 Gas absorption into a turbulent liquid. *Chem. Engng Sci.* **27,** 1035–1043.

LIMBERG, H. 1973 Warmeubergang an Turbulente and Laminare Rieselfilme. *Int. J. Heat Mass Transfer* **16,** 1691–1702.

LUCAS, K. & MOSER, B. 1979 Laminar film condensation of pure vapours in tubes. *Int. J. Heat Mass Transfer* **22,** 431–435.

MCADAMS, W. H. 1954 *Heat Transmission*, 3rd edn, Chap. 13. McGraw-Hill, New York.

MILLS, A. F. & CHUNG, D. K. 1973 Heat transfer across turbulent falling films. *Int. J. Heat Mass Transfer* **16,** 694–696.

MOCHIZUKI, S., YAGI, Y., TADANO, R., & YANG, W. J. 1984 Convective filmwise condensation of nonazeotropic binary mixtures in a vertical tube. *ASME Jl Heat Transfer* **106,** 531–538.

ROHSENOW, W. M., WEBBER, J. H. & LING, A. T. 1956 Effect of vapor velocity on laminar and turbulent film condensation. *Trans. ASME* **78,** 1637–1643.

SEBAN, R. A. 1954 Remarks on film condensation with turbulent flow. *Trans. ASME* **76,** 299–303.

SEBAN, R. A. & FAGHRI, A. 1976 Evaporation and heating with turbulent falling liquid films. *Trans. ASME Jl Heat Transfer* **98C,** 315–318.

SHAH, M. M. 1979 A general correlation for heat transfer during film condensation inside pipes. *Int. J. Heat Mass Transfer* **22,** 547–555.

SOLIMAN, M., SCHUSTER, J. R. & BERENSON, P. J. 1968 A general heat transfer correlation for annular flow condensation. *ASME Jl Heat Transfer* **90,** 267–276.

YIH, S. M. & LIU, J. L. 1984 Falling liquid films with or without interfacial shear. *AIChE Jl* **29,** 903–909.